Hydrogen Storage in Crystaline Structures

Diego De Gusem & Mylo Gijbels[1]

Keywords: Hydrogen storage, Density Functional Theory (DFT), Stability assesment, Li_3AlH_6, Renewable energy, Computational material physics

ABSTRACT

In this paper a computational analysis of hydrogen storage in crystal structures was performed. This was done by analysing the following *element combinations* X-Al-H where X=Li or K and Na-Y-H where Y=Al or Ga. For each of these combinations 5 crystals were constructed and analysed. This was done by calculating the energy of the relaxed crystal using Density Functional Theory (DFT) and calculating the pressure of H_2 inside these crystals. A transition between each of these crystals can occur using another of the 5 crystals in the composition or decomposition. Using the information of the energy of the different crystal structures it can be seen which of these crystals is the most stable and the amount of hydrogen it can store. From all the crystals that were researched only 2 were unstable and thus unfeasible, namely $LiAlH_4$ and $Li_5Al_3H_{14}$. All other crystals were stable where Li_3AlH_6 was chosen as the most suitable for hydrogen storage.

1. Introduction

Due to the rising population of the planet and the continuous demand for increasing computational power, there is a demand for more energy. This means that an ever-increasing amount of energy needs to be generated which is often in conflict with environmental concerns such as climate change. A possible solution to this problem is the large scale implementation of green energy sources like wind or solar power. However, these technologies share a common problem, power cannot be generated at a consistent rate as they are dependent on external uncontrollable factors. For instance in order to generate solar power the sun is needed and windmills only work when there is wind. In order to combat the problem of this dependability, a solution could be to store the energy when an excess is generated. A promising solution is the storage of energy in Hydrogen because of its ready availability and sustainable nature [1, 2]. Using gaseous hydrogen brings its own difficulties like its highly flammable nature. In this paper hydrogen storage in crystalline structures will be studied in order to look for possible energy storage alternatives. This will be done for 25 different crystals with comparable structures as the AlH_3, $NaAlH_4$, $Na_5Al_3H_{14}$, Na_3AlH_6 and NaH crystals.

2. Computational Method

All calculations performed in this report were made using the QuantumESPRESSO software.

2.1. Convergence Testing

In order to be certain that the calculations that were performed gave meaningful results, a convergence test was performed. This is done to ensure that the calculations were not performed on an unstable system, thereby minimizing the chance that the obtained results are merely noise measurements. For this convergence testing we iterated over different values of the following 3 parameters: k-mesh, ecutwfc and ecutrho. Next, we observed when the values were sufficiently converged based on some criteria. These criteria were that the forces should be converged up to 3mRy/au and that the components of the stress tensor should be converged up to 3kbar.

2.2. Geometry Optimisation

After the converged values for the parameters were determined, the crystal itself needed to be optimised. This is done by, in turn, varying the volume of the unit cell, the shape of the cell and the positions of the individual atoms in the unit cell. This is done similarly to the previous optimisation by varying one parameter and looking at the forces and pressures in the crystal. The value of the parameter that minimises these quantities is taken

[1] With thanks to Yashraj Kumar Singh and Olalekan Christian Olatunde for helping to get the project started.

to be the value the crystal would take in the real world. Using the "vc-relax" command in the input files, QuantumESPRESSO did this automatically.

2.3. Phase Diagram

Once the crystals were geometry optimised, a phase diagram could be made. This was done by making a graph that compared the energy of a crystal to its components, the resulting energy is the formation energy. If the formation energy is lower than 0, the crystal is stable and a possible candidate for hydrogen storage. If not, then the crystal is unstable and will decay to more stable structures.

3. Results

3.1. $Na-Al-H$

$NaAlH_4 + Na_5Al_3H_{14} + Na_3AlH_6 \leftrightarrow 5AlH_3 + 9NaH$

3.1.1. Properties

Table 1 shows properties of the used crystal structures. The degrees of freedom in the table are the added degrees of freedom from the Wyckoff positions and the shape of the crystal. The pressure was calculated using the ideal gas law, $P = \frac{Nk_BT}{V}$, where N is the amount of H_2 molecules, k_B is the Boltzman constant, V is the volume and T is the temperature chosen to be 293 K. The other constants used can be found on https://next-gen.materialsproject.org/.

3.1.2. Convergence Testing

The crystal chosen for the convergence tests was $NaAlH_4$. This crystal was chosen since it consists of the least amount of atoms, which makes it computationally the fastest while also containing all the elements that were used in these crystals. The result of the convergence tests can be seen in figures 1, 2 and 3. Based on these plots the k-mesh was set to $(4,4,4,0,0,0)$, ecutwfc to 56 and ecutrho to 224.

3.1.3. Phase Diagram

Using the values previously found for the k-mesh, ecutwfc and ecutrho, each crystal was geometry optimised and a phase diagram was created. The result for these crystals can be found in figure 13. It is clear that the geometry optimisation lowers the energy of the crystals a little bit. This suggests that the original crystals were almost completely optimised. This diagram states that $NaAlH_4$ is the most stable crystal and can contain almost as much H_2 as the other crystals. Therefore, we would opt to use this crystal for hydrogen storage.

3.2. $K-Al-H$

3.2.1. Properties

For these elements, the same crystal-types were generated as with $Na-Al-H$. Now these are AlH_3, $KAlH_4$, $K_5Al_3H_{14}$, K_3AlH_6 and KH.
This was done by replacing each Na atom by a K atom. This means that all features will remain the same as in table 1, except for the H_2 pressure. The pressure, after the geometry optimisation, is listed in table 2.

Table 2: Properties of $K-Al-H$.

Formula	H_2 Pressure [MPa]
AlH_3	130.28
$KAlH_4$	86.72
$K_5Al_3H_{14}$	93.60
K_3AlH_6	77.44
KH	44.43

3.2.2. Convergence Testing

To do the convergence testing, the same procedure was applied as before. Again the crystal with the least amount of atoms, $KAlH_4$, was chosen for this test. The resulting k-mesh, ecutwfc and ecutrho were $(5,5,5,0,0,0)$, 66, 330 respectively. The graphs for these tests can be seen in figures 4, 5 and 6.

3.2.3. Phase Diagram

Using these parameters, the system was fully geometry optimised and the resulting phase diagram can be seen in figure 14. Just like before, $KAlH_4$ is the most stable crystal while also having a H_2 pressure comparable to the other crystals. That is why we would chose this crystal for hydrogen storage.

3.3. $Li-Al-H$

In this section we once again look at the same crystal structure but this time we replaced the original Na atom with Lithium. This gives the following structures: AlH_3, $LiAlH_3$, $Li_5Al_3H_{14}$, Li_3AlH_6 and LiH. These retain the same amount of atoms in the unit cell and degrees of freedom as the original crystals.
The pressures of H_2 of the relaxed crystals can be found in table 3.

Table 3: Properties of $Li-Al-H$.

Formula	H_2 Pressure [MPa]
AlH_3	130.28
$LiAlH_4$	151.00
$Li_5Al_3H_{14}$	151.66
Li_3AlH_6	146.77
LiH	124.46

Table 1: Properties of $Na-Al-H$.

Formula	Atoms per Primitive Cell	Degrees of Freedom	H_2 Pressure [MPa]
AlH_3	16	1	134.12
$NaAlH_4$	12	4	120.62
Na_5Al3H_{14}	44	8	124.60
Na_3AlH_6	20	15	109.60
NaH	2	0	74.42

3.3.1. Convergence Testing

The same convergence tests as before where performed here. This time on the $LiAlH_4$ the results of which can be seen in figure 7 - 9. From these results the following parameters were chosen: ecutwfc = 75, ecutrho = 300 and a k-mesh of $(4,4,4,0,0,0)$.

3.3.2. Phase Diagram

Using the parameters mentioned in the previous section a geometry optimisation is performed on the crystals. From these relaxed crystals a phase diagram was constructed, the result can be seen in figure 15. This diagram has a significantly different form from the others that where found. Both $LiAlH_4$ and $Li_5Al_3H_{14}$ have an energy greater than zero. This means that $LiAlH_4$ and $Li_5Al_3H_{14}$ are unstable configurations of the crystal, and thus not suited for the hydrogen storage application. The crystal that was selected as a candidate for the storage application in this case was Li_3AlH_6.

3.4. $Na-Ga-H$

3.4.1. Properties

Again the same crystal structures were chosen as for $Na-Al-H$. This means that the crystals for GaH_3, $NaGaH_4$, $Na_5Ga_3H_{14}$, Na_3GaH_4 and NaH were constructed. This was done by replacing the Al atom with Ga in the files of the $Na-Al-H$ crystals. Again the properties of the crystals remained the same as in table 1, except for the H_2 pressure. The pressure was calculated after optimising the geometry and is listed in table 4. Due to an unknown reason the geometry optimisation for the $Na_5Ga_3H_{14}$ crystal could not be performed in a correct way. As a result, no statements can be made for this structure.

Table 4: Properties of $Na-Ga-H$.

Formula	H_2 Pressure [MPa]
GaH_3	119.68
$NaGaH_4$	109.98
Na_3GaH_6	103.33
NaH	71.44

3.4.2. Convergence Testing

The same convergence tests were performed as with $Na-Al-H$, $Li-Al-H$ and $K-Al-H$. This time choosing $NaGaH_4$ for the tests, because it has the least amount of atoms. The tests resulted in a k-mesh of $(5,5,5,0,0,0)$, ecutwfc of 86 and ecutrho of 258. See figures 10, 11 and 12 for the plots of this test.

3.4.3. Phase Diagram

After optimising the geometry, the phase diagram in figure 16 was found. In this figure it is clear that $NaGaH_4$ is the most stable element while also having the highest H_2 pressure. That is why we would choose this crystal for hydrogen storage.

4. Conclusion

After the geometry optimisation from all $Na-Al-H$, $K-Al-H$, $Li-Al-H$ and $Na-Ga-H$ crystals, we concluded that $NaAlH_4$, $KAlH_4$, Li_3AlH_6 and $NaGaH_4$ are the most stable. The H_2 pressure for each of these crystals is given by 120.62MPa, 86.72MPa, 146.77MPa and 109.98MPa respectively. This makes sense, because the potassium element is bigger than sodium and lithium and thus requires more space, while the reverse is true for the lithium crystal. It can also be seen that gallium requires more space than aluminium, which also makes sense. From the results that were found in this project, we can conclude that the Li_3AlH_6 crystal can store the most hydrogen while still maintaining a stable crystal. That is why, based on the crystals tested here, we would propose to use Li_3AlH_6 for hydrogen storage.

REFERENCES
References

[1] Kumar, A., Muthukumar, P., Sharma, P., & Kumar, E. A. (2022). Absorption based Solid state Hydrogen Storage System: a review. Sustainable Energy Technologies and Assessments, 52, 102204. https://doi.org/10.1016/j.seta.2022.102204

[2] Prasad, J. S., & Muthukumar, P. (2022). Performance and energy efficiency of a solid-state hydrogen storage system: an experimental study on LA0.7CE0.1CA0.3NI5. Applied Thermal Engineering, 216, 119030. https://doi.org/10.1016/j.applthermaleng.2022.119030

A. Appendix Convergence Tests

A.1. $Na - Al - H$

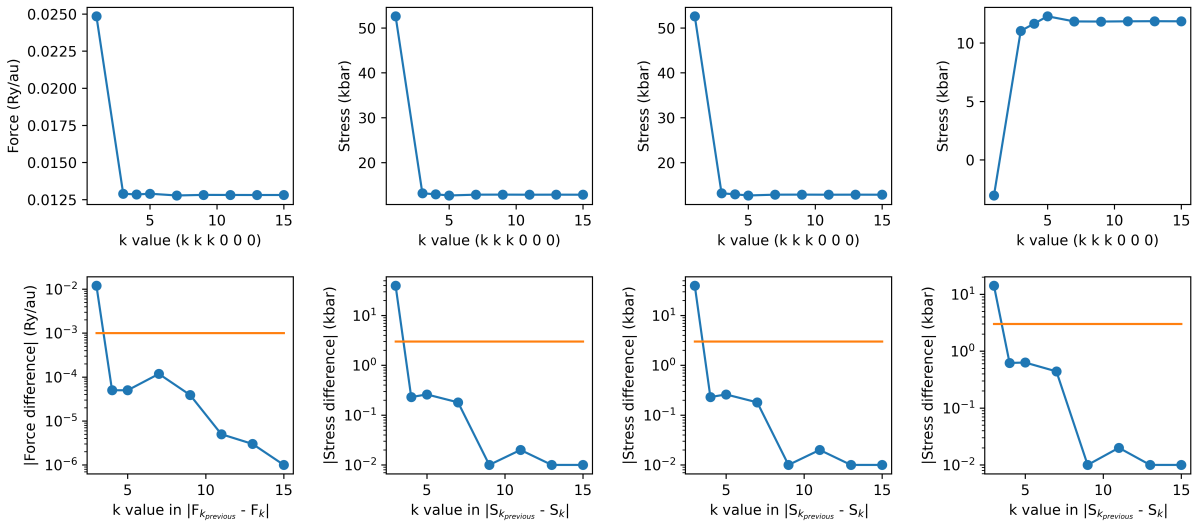

Figure 1: Convergence test for the k-mesh for $NaAlH_4$. The top row shows the total force and stress tensor components in function of the k-value. The bottom row has the difference between two consecutive k-values and the orange line represents the convergence criterion.

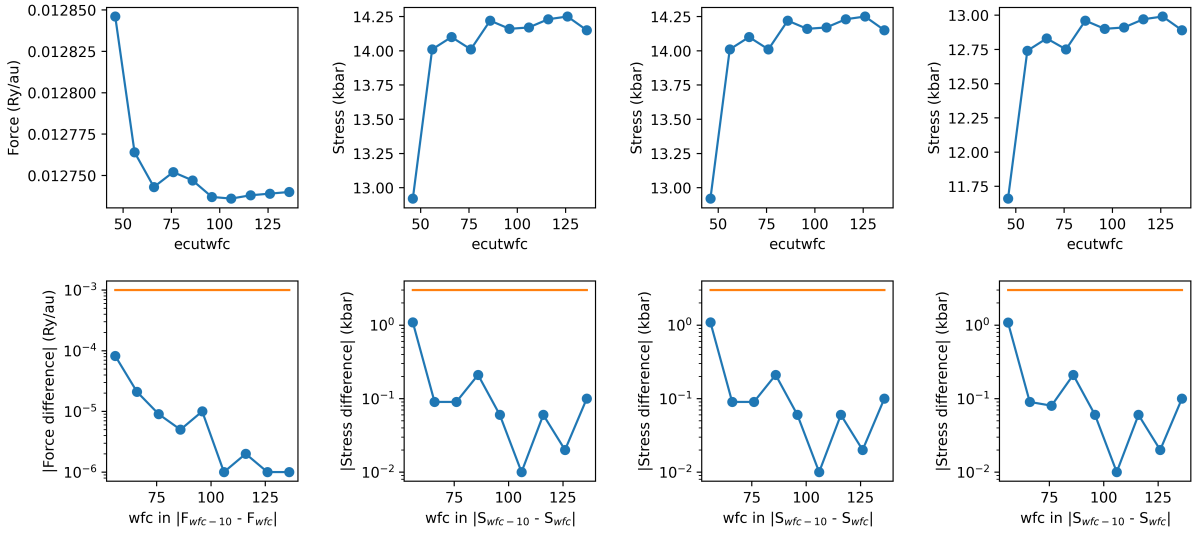

Figure 2: Convergence test for the ecutwfc for $NaAlH_4$. The top row shows the total force and stress tensor components in function of ecutwfc. The bottom row has the difference between two consecutive ecutwfc-values and the orange line represents the convergence criterion.

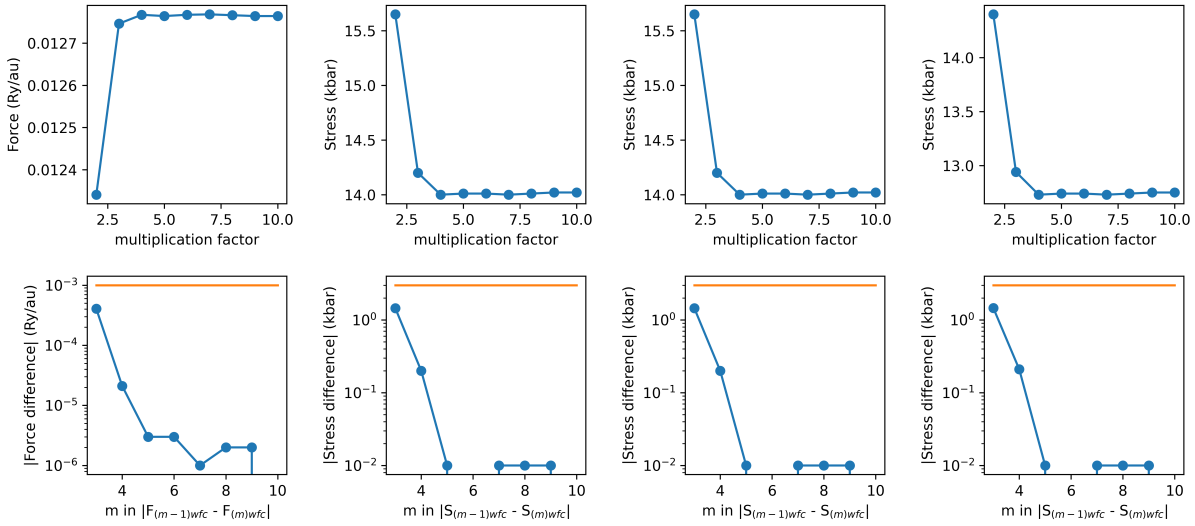

Figure 3: Convergence test for the ecutrho for $NaAlH_4$. Ecutrho is equal to ecutwfc times a multiplication factor. The top row shows the total force and stress tensor components in function of the multiplication factor. The bottom row has the difference between two consecutive multiplication-values and the orange line represents the convergence criterion.

A.2. $K-Al-H$

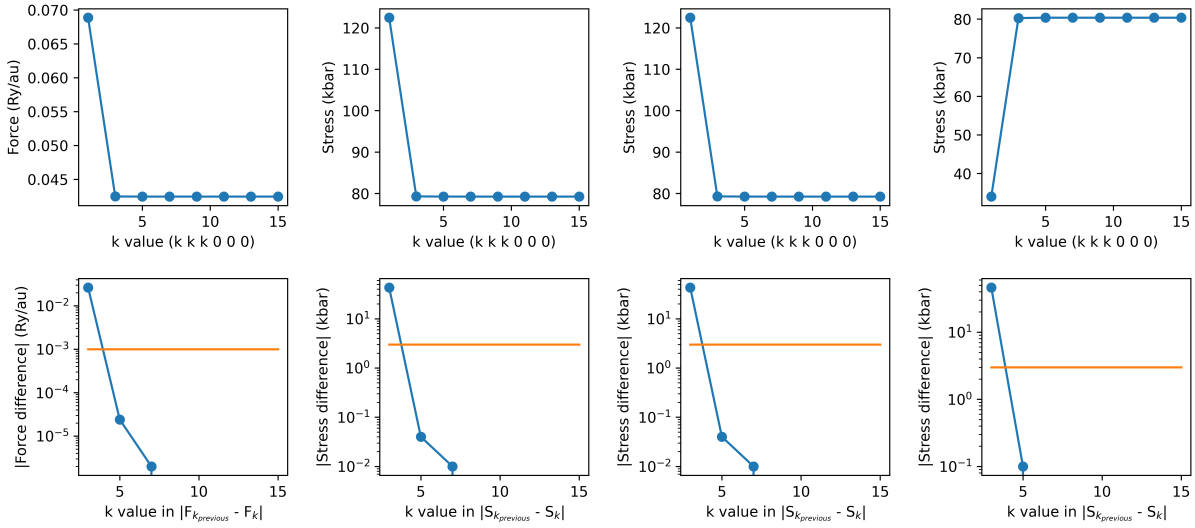

Figure 4: Convergence test for the k-mesh for $KAlH_4$. The top row shows the total force and stress tensor components in function of the k-value. The bottom row has the difference between two consecutive k-values and the orange line represents the convergence criterion.

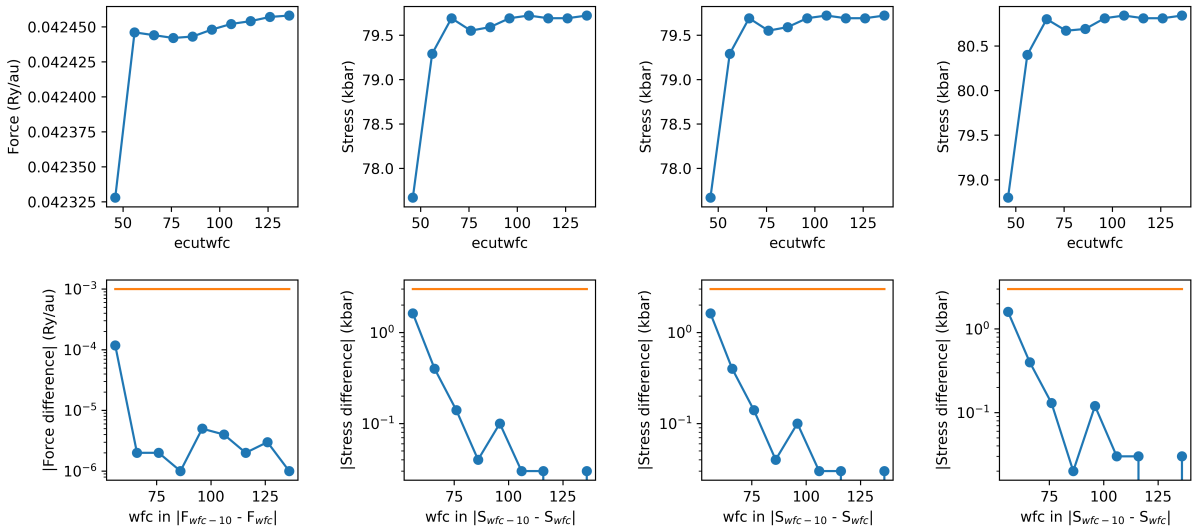

Figure 5: Convergence test for the ecutwfc for $KAlH_4$. The top row shows the total force and stress tensor components in function of ecutwfc. The bottom row has the difference between two consecutive ecutwfc-values and the orange line represents the convergence criterion.

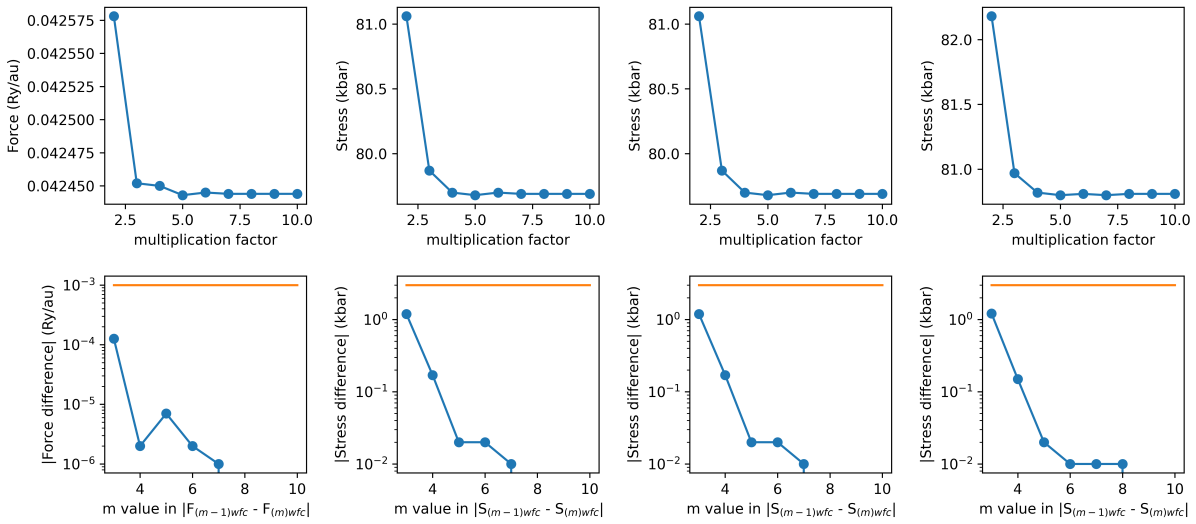

Figure 6: Convergence test for the ecutrho for $KAlH_4$. Ecutrho is equal to ecutwfc times a multiplication factor. The top row shows the total force and stress tensor components in function of the multiplication factor. The bottom row has the difference between two consecutive multiplication-values and the orange line represents the convergence criterion.

A.3. $Li - Al - H$

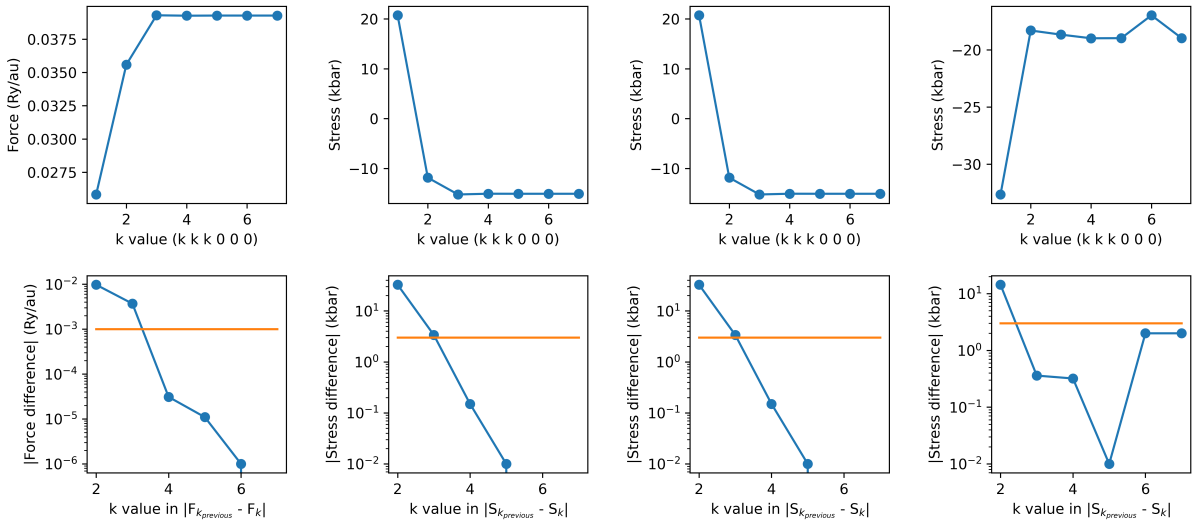

Figure 7: Convergence test for the k-mesh for $LiAlH_4$. The top row shows the total force and stress tensor components in function of the k-value. The bottom row has the difference between two consecutive k-values and the orange line represents the convergence criterion.

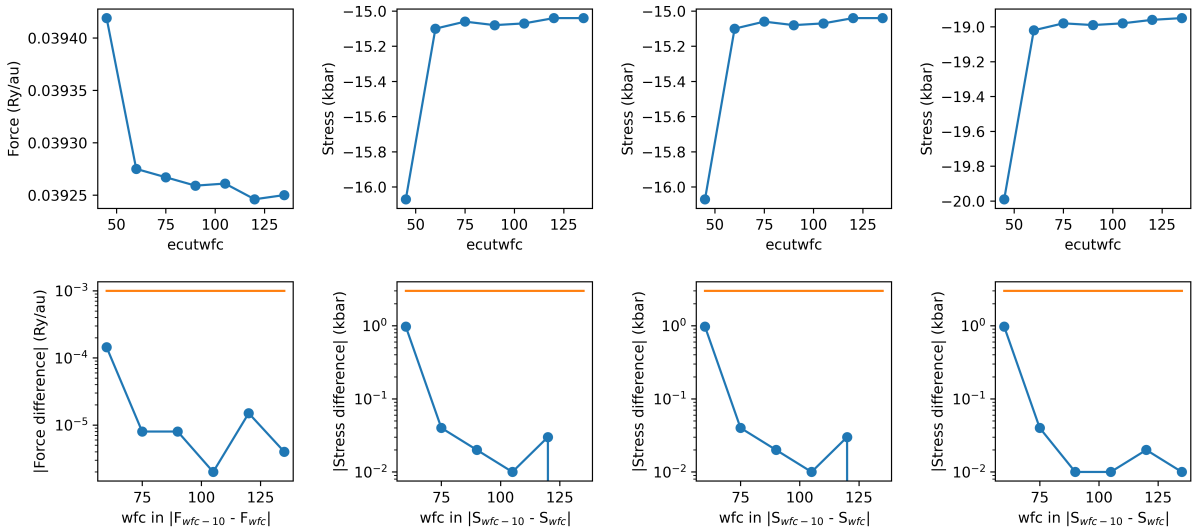

Figure 8: Convergence test for the ecutwfc for $LiAlH_4$. The top row shows the total force and stress tensor components in function of ecutwfc. The bottom row has the difference between two consecutive ecutwfc-values and the orange line represents the convergence criterion.

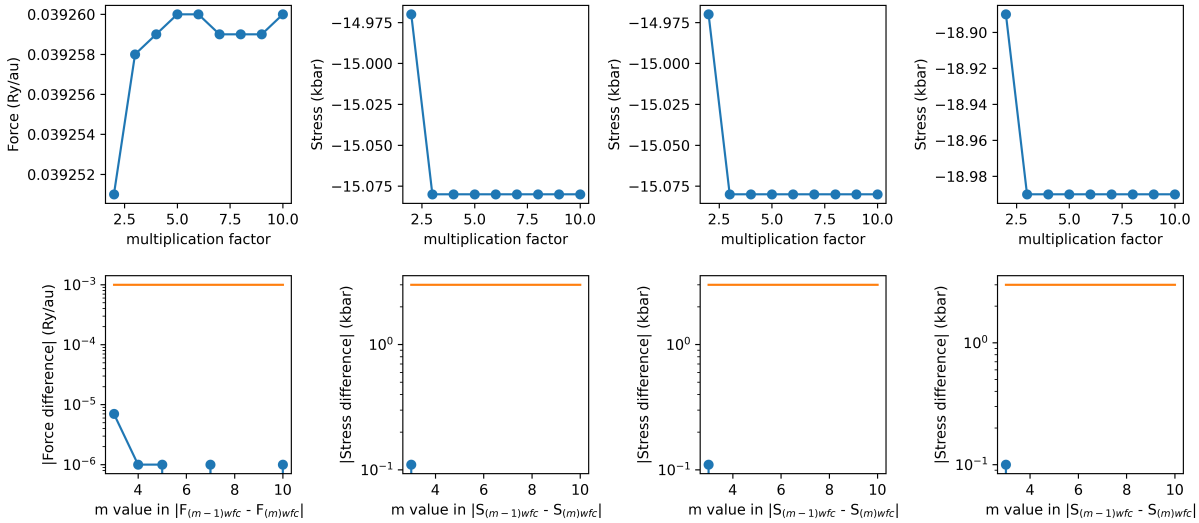

Figure 9: Convergence test for the ecutrho for $LiAlH_4$. Ecutrho is equal to ecutwfc times a multiplication factor. The top row shows the total force and stress tensor components in function of the multiplication factor. The bottom row has the difference between two consecutive multiplication-values and the orange line represents the convergence criterion.

A.4. $Na - Ga - H$

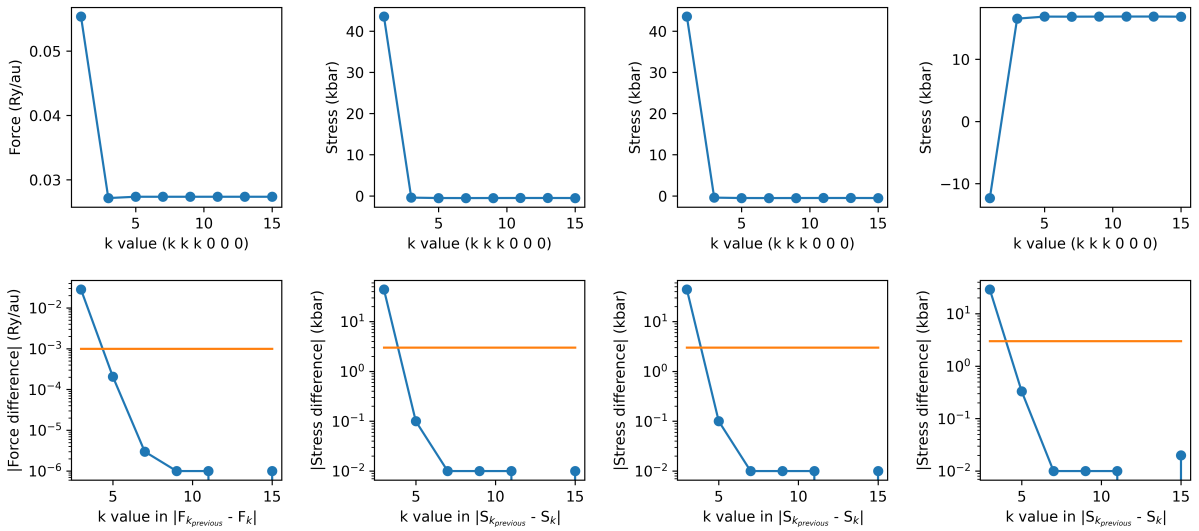

Figure 10: Convergence test for the k-mesh for $NaGaH_4$. The top shows row the total force and stress tensor components in function of the k-value. The bottom row has the difference between two consecutive k-values and the orange line represents the convergence criterion.

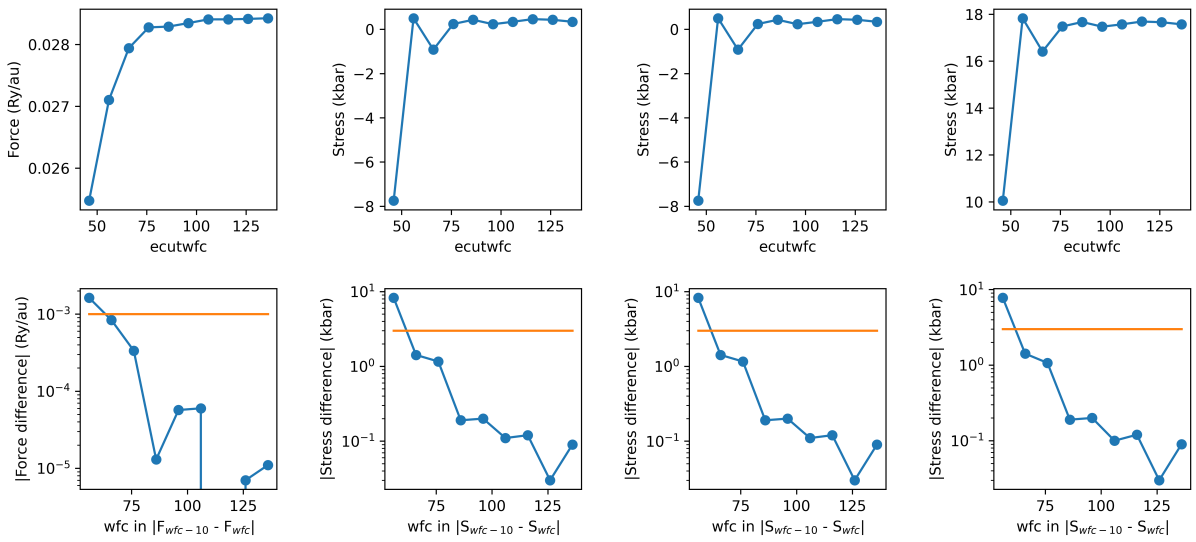

Figure 11: Convergence test for the ecutwfc for $NaGaH_4$. The top row shows the total force and stress tensor components in function of ecutwfc. The bottom row has the difference between two consecutive ecutwfc-values and the orange line represents the convergence criterion.

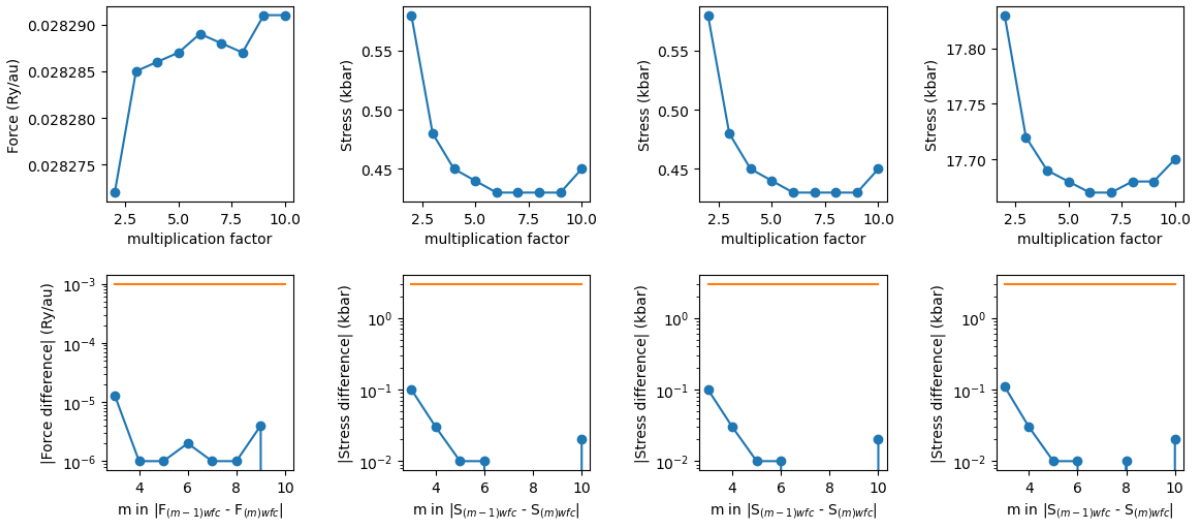

Figure 12: Convergence test for the ecutrho for $NaGaH_4$. Ecutrho is equal to ecutwfc times a multiplication factor. The top row shows the total force and stress tensor components in function of the multiplication factor. The bottom row has the difference between two consecutive multiplication-values and the orange line represents the convergence criterion.

B. Appendix Phase Diagrams

B.1. $Na - Al - H$

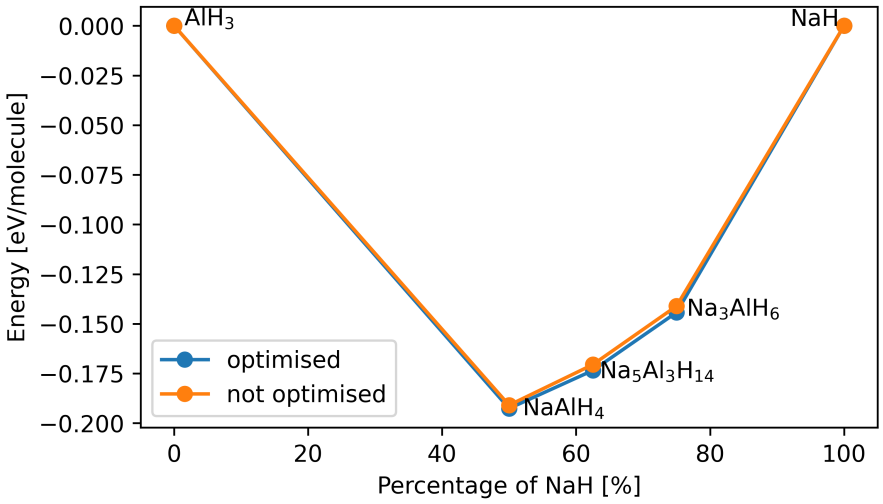

Figure 13: The phase diagram for $Na - Al - H$. The orange curve represents the diagram without the geometry optimisation, while the blue curve is with the optimisation.

B.2. $K - Al - H$

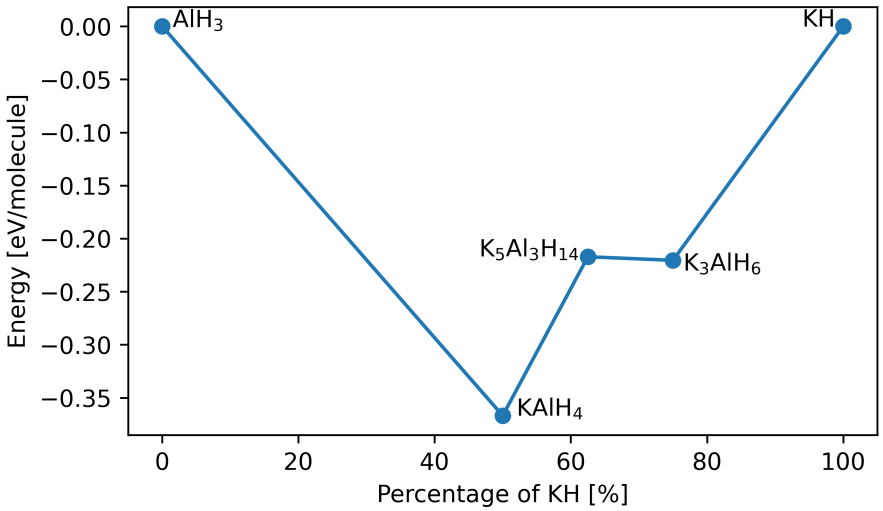

Figure 14: The phase diagram for $K - Al - H$.

B.3. $Li - Al - H$

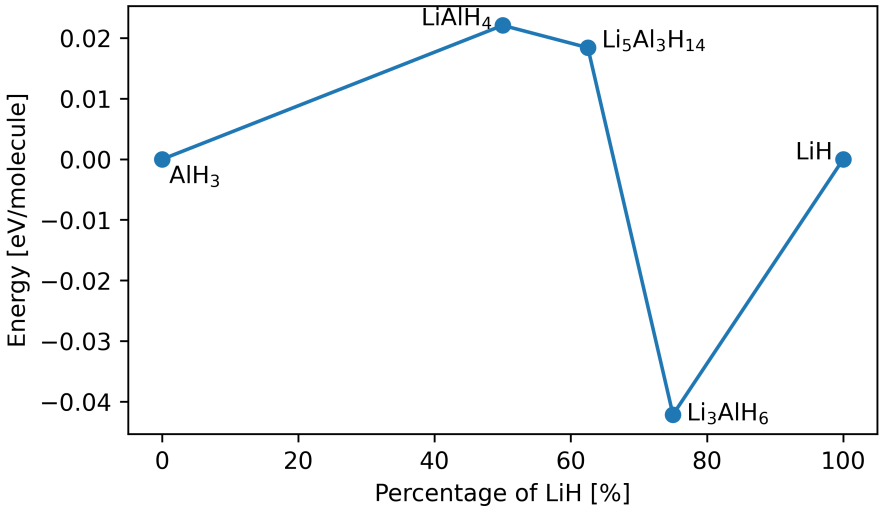

Figure 15: The phase diagram for $K - Al - H$.

B.4. $Na - Ga - H$

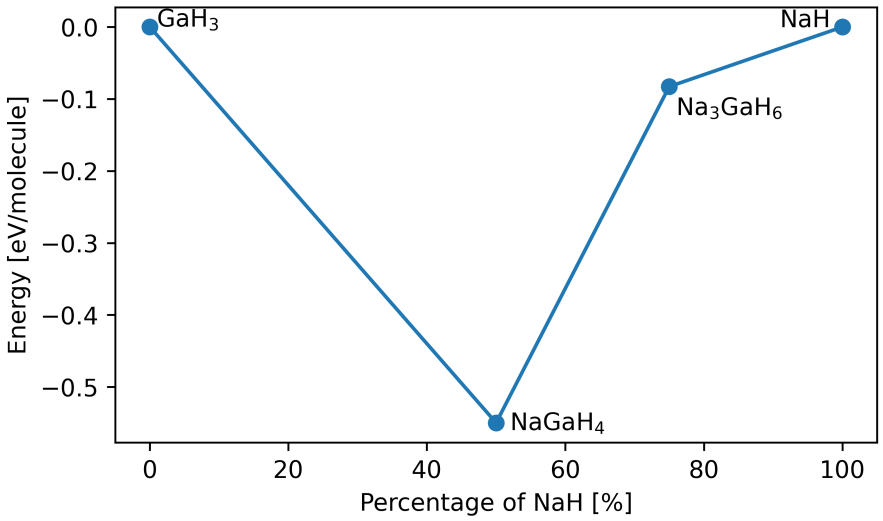

Figure 16: The phase diagram for $Na - Ga - H$.